POLITECNICO DI TORINO
Repository ISTITUZIONALE

Modeling of single-mode high-power VCSEL arrays

(Article begins on next page)

09 May 2024

Modeling of single-mode high-power VCSEL arrays

Valerio Torrelli*†, Alberto Tibaldi*†, Francesco Bertazzi*†,
Michele Goano*†, Pierluigi Debernardi†

* Dipartimento di Elettronica e Telecomunicazioni, Politecnico di Torino, Corso Duca degli Abruzzi 24, 10129 Torino, Italy
† CNR-IEIIT, Corso Duca degli Abruzzi 24, 10129 Torino, Italy
E-mail: valerio.torrelli@polito.it

Abstract—In this work we investigate different architectures to realize a single-mode VCSEL array for high power applications. This is done by simulating a large active-area VCSEL with either a metallic or a grating-relief-based patterning at the outcoupling aperture. The investigated designs are compared, highlighting possible strategies to improve the fiber coupling by improving the far field (FF) profile. This contribution also presents a satisfactory match between the simulations and the FF experimental data obtained from the measurements of a VCSEL array structure.

I. INTRODUCTION

Vertical-cavity surface-emitting lasers (VCSELs) are now used for a large variety of applications, ranging from data communication [1] to sensing [2]. Among these, the employment of VCSELs for high power single-mode scopes has always been a tricky task. One possibility is represented by VCSEL arrays, however, with such structures, it is hard to obtain a single mode emission. When dealing with standard VCSELs, a possible way to ensure a single lasing mode with a stable polarization is to use a sub-wavelength grating relief on top of the laser [3]–[5], relying on a $\lambda/4$ relief etched in an antiphase cap layer. In this way only the fundamental mode with the desired polarization is promoted, because the higher order modes experience the higher losses outside the relief, where antiphase reflectivity occurs.

In this work, we study a large active area VCSEL, which would normally lead to multi-mode emission, patterning its outcoupling facet with a metal array or grating reliefs as mode selectors. In this way we achieve higher power single mode emission.

The simulations are performed by means of our in-house 3D vectorial Vcsel ELectroMagnetic code VELM, already proven effective for a variety of VCSEL structures including 2D metal arrays and grating reliefs [6]–[13].

II. RESULTS AND DISCUSSION

As a preliminary validation, we simulated a VCSEL array structure featuring a rectangular active area of 30 μm along the x direction and 4 μm along the y direction and a linear array of 8 grating reliefs on top acting as mode selector for the mode with 7 nodes along x and no nodes along y (for a general idea of the transverse geometry, see Fig. 2, top). Validation is performed against the experimental FF data, measured at 10 mA, which we compared with the numerical results obtained for a slightly reduced active side (28 μm instead of 30 μm along x) to account for thermal lensing, not yet included in
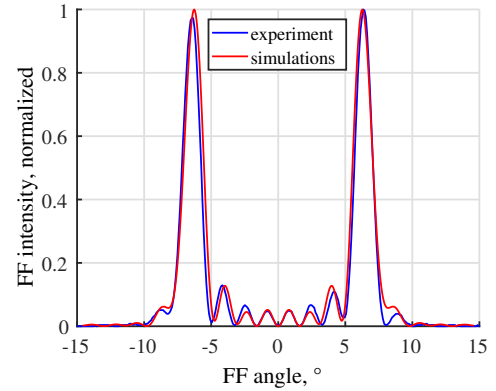

Fig. 1. Experimental and simulated FF profiles against the FF angle in the x direction of a large area VCSEL with 8 grating reliefs on top.

the simulations. The experimental and simulated FF profiles along the x direction are reported in Fig. 1. The good fit with the two peaks, as well as with the grating lobes, demonstrates the accuracy of our simulations.

At this point, we proceed with the simulation of an active area of 26×6 μm^2, illustrating the array design. By putting at the outcoupling aperture of this structure only a 50 nm thick platinum contact with a larger aperture than the active area (like the one at Fig. 2, top), the resulting modes are extremely close in threshold gain (multi-mode emission). Two of the resulting modes are shown in Fig. 2 (bottom), which we can identify as the fundamental mode with threshold gain of 649.6 cm^{-1} (left) and the one we would like to select (right) with threshold gain of 704.5 cm^{-1}. Exploiting the spatial distribution of the mode with 4 nodes, we can design the mode selectors so that they resemble its geometry. We could either trace out a metal array (design A) following the approach of [11], a grating relief array (design B) or, to improve the FF profile, we could try a combination of the two methods (design C) following [11]. With the latter, three reliefs corresponding to the positive field spots of Fig. 2 (bottom, right) are used as mode selectors. On the other hand, the metal is used to inhibit the second and fourth spot at the output section, in order to limit the interference effect in the FF due to the sign change, resulting in a profile where the middle portion of the field is not suppressed, better in the view of fiber coupling. In these three designs, the metal is still made out of a 50 nm thick platinum layer. The favoured modes in the three cases
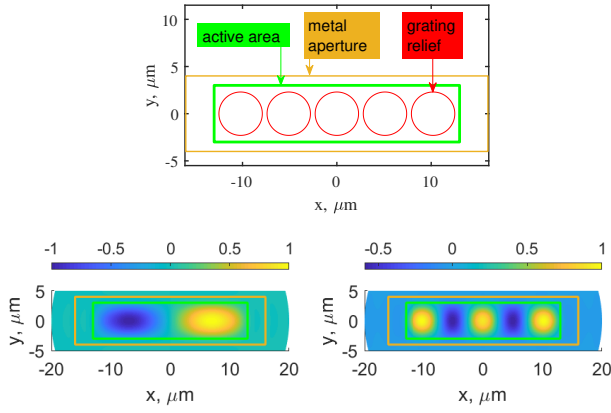
Fig. 2. Possible patterning at the outcoupling facet with corresponding color code (top). Dominant field component of the mode with the lowest threshold gain (bottom, left) and mode with 4 nodes along x (bottom, right) for the test structure without arrays on top, evaluated at the output section of the laser.
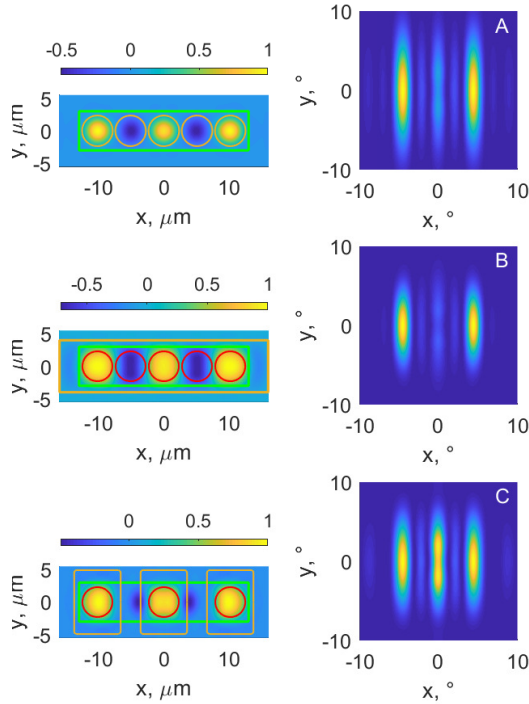
are reported in Fig. 3.

Fig. 3. Dominant field components of the favoured modes at the output section of the laser and corresponding FF profiles for the designs A (top), B (middle) and C (bottom). All of the designs work as mode selectors.

In Tab. I we summarize the results for the three designs, in terms of threshold gains of the lasing mode and the one just above, i.e., $G_{th}^{(0)}$ and $G_{th}^{(1)}$. We also provide the corresponding outcoupling efficiency η, defined as the ratio of the emitted power to the power provided by the quantum wells.

The effect of the metallization is a reduction of the threshold gain as well as a reduction of the outcoupling efficiency. The grating relief array yields an increased threshold gain, because the gratings and the antiphase mirror worsen the optimal in-

design	$G_{th}^{(0)}$, cm^{-1}	$G_{th}^{(1)}$, cm^{-1}	η	superior mode
A	916	1073	0.52	4 field spots
B	1149	1448	0.86	10 field spots
C	1113	1414	0.65	4 field spots

TABLE I
MAIN CHARACTERISTICS OF THE THREE ARRAY DESIGNS.

phase design. This is the price to pay to achieve polarization and transverse mode control at the same time. However, it provides a very good modal discrimination between the favoured and the first superior mode, not to mention the polarization control. Focusing on the profiles in Fig. 3, one can notice that the inhibition of the negative field at the output section is the key to obtain a central peak in the FF. In the design C an increase of the metal thickness would correspond to a FF profile with a more dominant central spot due to the stronger inhibition of the negative field. This, however, would lead to an even lower η.

In conclusion, the metal array solution works as mode selector and provides a good carrier injection, but it does not provide a control on the polarization and has a lower outcoupling efficiency. On the other hand the grating relief array solution ensures the polarization control, with a higher threshold gain and a slightly worse carrier injection (especially true for 2D arrays). Finally, the combined solution ensures the polarization control, has lower thresholds and a good carrier injection and it provides a better fiber coupling due to the FF profile improvement, at the cost of a reduced outcoupling efficiency.

REFERENCES

[1] A. Tibaldi, F. Bertazzi, M. Goano, R. Michalzik, P. Debernardi, *IEEE Journal of Selected Topics in Quantum Electronics* **25**, 1 (2019).
[2] G. K. Veerabathran, S. Sprengel, A. Andrejew, M.-C. Amann, *Appl. Phys. Lett.* **110**, 071104 (2017).
[3] K. J. Ebeling, R. Michalzik, H. Moench, *Japanese Journal of Applied Physics* **57**, 08PA02 (2018).
[4] T. Pusch, *et al.*, *Electronics Letters* **55**, 1055 (2019).
[5] C. Fuchs, *et al.*, *IEEE journal of quantum electronics* **43**, 1227 (2007).
[6] G. Bava, P. Debernardi, L. Fratta, *Physical Review A* **63**, 023816 (2001).
[7] P. Debernardi, G. P. Bava, *IEEE Journal of selected topics in quantum electronics* **9**, 905 (2003).
[8] P. Debernardi, R. Orta, T. Grundl, M.-C. Amann, *IEEE Journal of Quantum Electronics* **49**, 137 (2012).
[9] A. Tibaldi, *et al.*, *Optical and Quantum Electronics* **51**, 1 (2019).
[10] A. Gullino, A. Tibaldi, F. Bertazzi, M. Goano, P. Debernardi, *Applied Sciences* **11**, 6908 (2021).
[11] P. Debernardi, G. P. Bava, F. M. di Sopra, M. B. Willemsen, *IEEE journal of quantum electronics* **39**, 109 (2003).
[12] P. Debernardi, *IEEE journal of quantum electronics* **45**, 979 (2009).
[13] P. Debernardi, *et al.*, *IEEE Journal of Quantum Electronics* **52**, 1 (2016).